Enhanced differentiation of functional human T cells in NSGW41 mice with tissue-specific expression of human interleukin-7.

Emilie Coppin[1,2*], Bala Sai Sundarasetty[3*§], Susann Rahmig[1,2], Jonas Blume[4], Nikita A. Verheyden[3], Franz Bahlmann[5], Sarina Ravens[4], Undine Schubert[9,10], Janine Schmid[9,10], Stefan Ludwig[11], Constantin von Kaisenberg[6], Alexander Platz[7], Ronald Naumann[8], Barbara Ludwig[9,10], Immo Prinz[4], Claudia Waskow[1,2,9,12$], Andreas Krueger[3$]

[1] Regeneration in Hematopoiesis, Institute for Immunology, TU Dresden, Dresden, Germany
[2] Immunology of Aging, Leibniz Institute on Aging - Fritz Lipmann Institute, Jena, Germany.
[3] Institute for Molecular Medicine, Goethe University Frankfurt am Main, Germany.
[4] Institute of Immunology, Hannover Medical School, Hannover, Germany.
[5] Department of Obstetrics and Gynecology, Bürgerhospital Frankfurt, Germany.
[6] Department Obstetrics, Gynecology and Reproductive Medicine, Hannover Medical School, Hannover, Germany.
[7] DKMS Cord Blood Bank, Dresden, Germany.
[8] Max-Planck Institute of Molecular Cell Biology and Genetics, Dresden, Germany.
[9] Department of Medicine III, Technical University Dresden, Dresden, Germany.
[10] German Center for Diabetes Research (DZD e.V.), Neuherberg, Germany.
[11] Department of Visceral-, Thorax- and Vascular Surgery, Technical University Dresden, Dresden, Germany.
[12] Institute of Biochemistry and Biophysics, Faculty of Biological Sciences, Friedrich-Schiller-University Jena, Jena, Germany.

* same contribution first authors

[$] joint supervision

[§] Current address: Recombinant Technologies, CSL Behring GmbH, Marburg, Germany

Corresponding author

Claudia Waskow

Claudia.waskow@leibniz-fli.de

Leibniz-Institute on Aging, Beutenbergstrasse 11, 07745 Jena, Germany

Phone: +49 3641 656 707

Key words: human IL-7, BAC, humanized mice, NSGW41, T cell, thymus, HSPC, cord blood, thymopoiesis, T cell activation

Key points

1. Increased intrathymic human T cell differentiation in the absence of pathological lymphoproliferation in humanized NSGW41hIL7 mice.

2. Increased peripheral human T cell populations in NSGW41hIL7 mice making the analysis of human regulatory T cells in vivo feasible.

Abstract

Humanized mouse models have become increasingly valuable tools to study human hematopoiesis and infectious diseases. However, human T cell differentiation remains inefficient. We generated mice expressing human interleukin (IL-7), a critical growth and survival factor for T cells, under the control of murine IL-7 regulatory elements. After transfer of human cord blood-derived hematopoietic stem and progenitor cells, transgenic mice on the NSGW41 background, termed NSGW41hIL7, showed elevated and prolonged human cellularity in the thymus while maintaining physiological ratios of thymocyte subsets. As a consequence, numbers of functional human T cells in the periphery were increased without evidence for pathological lymphoproliferation or aberrant expansion of effector or memory-like T cells. We conclude that the novel NSGW41hIL7 strain represents an optimized mouse model for humanization to better understand human T cell differentiation *in vivo* and to generate a human immune system with a better approximation of human lymphocyte ratios.

Introduction

Humanized mouse models have emerged as indispensable tools for improving our understanding of human hematopoiesis and the human immune system. Typically, they are generated by transplanting human hematopoietic stem and progenitor cells (HSPCs) into mice (for review see [1]). NSGW41 mice carry the hypomorph W41 allele in the *Kit* gene, harbor the NOD-specific variant of the *Sirpa* gene, are T-, B- and NK-cell deficient based on null mutations in *Prkdc* and *Il2rg* genes, and allow for human donor stem cell engraftment in the absence of preconditioning [2, 3]. NSGW41 mice that are stably engrafted with human hematopoietic stem cell display continuous human hematopoiesis with increased myeloid [2, 4], megakaryocytic and erythroid output compared to irradiated NSG recipient mice [5, 6].

The introduction of human genes to overcome selective deficiencies in human hematopoiesis has resulted in further improvement of humanized mouse models. Thus, mice expressing human cytokines, including a combination of SCF, GM-CSF, and IL-3 (NSG-SGM3) or M-CSF, IL-3, GM-CSF, and thrombopoietin (MISTRG) show improved myelopoiesis [7, 8]. Mice carrying a knock-in of human IL-6 show improved B-cell development and function [9].

Efficient differentiation of human T cells remains a challenge in humanized mice and we have focused on interleukin-7 (IL-7) to improve that situation. Patients with mutations in the *IL7RA* gene suffer from profound T–B+NK+ severe combined immunodeficiency [10]. In mice, loss of the *Il7ra* gene results in combined B and T-cell lymphopenia, pointing towards critical cross-species differences [11, 12]. *In vitro*, murine (m)IL-7 was 100-fold less potent to expand and differentiate human T-cell progenitors when compared to human (h)IL-7 [13]. Given its role as key factor for lymphocyte survival and proliferation [10-13], unrestricted supply of IL-7 might result in unwanted effects including lymphoma generation [14]. Further, excessive amounts of mIL-7 limits T cell differentiation by interfering with Notch signaling [15, 16]. Here, we generated hIL-7 (hIL-7) BAC transgenic NSGW41 mice to improve T cell differentiation in humanized mice while simultaneously avoiding unwanted effects caused by excessive and spatially unrestricted availability of hIL-7.

Results and Discussion

To generate a mouse model with tissue-specific expression of human (h)IL-7, we inserted cDNA encoding *IL7* into a BAC containing regulatory elements of the murine

99 *Il7* locus (Fig. 1a). BAC transgenic mice were generated on the NOD background,
100 crossed into the NSGW41 strain [2] and termed NSGW41hIL7. NSGW41hIL7 mice
101 contain three copies of the BAC transgene and expressed hIL-7 mRNA and protein in
102 BM, spleen and thymus (Fig. 1b,c). Engraftment of human HSPCs and T cell
103 differentiation was determined at indicated time points after transplantation of $CD34^+$-
104 enriched cord blood cells into unconditioned NSGW41 or NSGW41hIL7 mice (Fig. 1d).
105 Blood from NSGW41 or NSGW41hIL7 mice contained comparable levels of human
106 hematopoietic cells peaking at 16-18 weeks after transplantation (Fig. 1e). However,
107 beginning at week 16 after transplantation frequencies of T cells among human $CD45^+$
108 cells were significantly increased in NSGW41hIL7 mice compared to NSGW41
109 recipients. Correspondingly, ratios of T and B cells increased progressively over time,
110 with T cells ultimately becoming the predominant lymphocyte population in blood of
111 NSGW41hIL7 mice (Fig. 1e,f). T/B ratios >1 are also observed in human blood.
112 Consistently, in spleens, human $CD45^+$ leukocytes were increased in NSGW41hIL7
113 mice compared to NSGW41 mice, which was mainly attributable to increased numbers
114 of T cells (Fig. S1a,b). The data indicate that expression of hIL-7 under control of
115 endogenous gene regulatory elements fosters T-cell differentiation in NSGW41hIL7
116 mice.
117
118 Next, we assessed whether elevated frequencies of peripheral human T cells in
119 NSGW41hIL7 mice were due to more efficient intrathymic T-cell differentiation.
120 Human $CD45^+$ cell numbers were 3.3-fold, 3.5-fold, and 21.2-fold higher in thymi from
121 NSGW41hIL7 mice at 15, 18, and 26 weeks after reconstitution, respectively (Fig. 2a).
122 Ratios of human CD4/CD8 double negative (DN), double positive (DP), and CD4 and
123 CD8 single positive (SP) thymocytes were comparable in both recipient lines 15 and
124 18 weeks after transplantation, indicating that ectopic expression of hIL-7 did not result
125 in aberrant T cell differentiation (Fig. 2b,c). NSGW41hIL7 but not NSGW41 thymi
126 predominantly contained DP thymocytes 26-32 weeks after transplantation. In
127 contrast, DN thymocytes constituted the major population in NSGW41 mice,
128 suggesting that hIL-7 supports human T cell differentiation for extended periods of time
129 in NSGW41hIL7 mice. A recently characterized combined knock-in of hIL-7 and hIL-
130 15 on the NSG background displayed massive skewing towards CD8 SP cells at the
131 expense of DP thymocytes [17], suggesting that tissue-specific expression of human
132 cytokines alone is insufficient to promote human T cell differentiation [18]. Consistent

133 with the T-lineage specific role of hIL-7 in human hematopoiesis, and confirming
134 specificity of transgenic expression of hIL-7, we observed no alterations in B-cell
135 differentiation in NSGW41hIL7 mice compared to NSGW41 (Fig. 2d, S2a,b). We
136 conclude that NSGW41hIL7 mice display improved and extended intrathymic T cell
137 differentiation from human cord blood-derived HSPCs, temporally coinciding with a
138 shift in T/B cell ratios in the periphery.
139
140 Elevated levels of human T-cell precursors in thymus suggested that the increased
141 frequencies of T cells in blood and spleen were largely reflecting increased thymic
142 output. However, hIL-7 might also alter peripheral homeostasis. To test this possibility
143 we further characterized peripheral T cell subsets in NSGW41hIL7 mice. $CD4^+$ and
144 $CD8^+$ T cell numbers in the blood were increased to comparable extent (Fig. 3a). Within
145 $CD4^+$ T cells, frequencies of naive T cells and Recent Thymic Emigrants (RTEs) and
146 effector T cells increased in NSGW41hIL7 mice compared to NSGW41 (Fig. 3b,S3).
147 Concomitantly, frequencies of effector memory T cells were reduced. In $CD8^+$ T cells,
148 a similar increase in naive and RTE and decrease in effector memory frequencies was
149 observed, whereas frequencies of T effector and central memory subsets remained
150 comparable to those detected in NSGW41 mice (Fig. 3b, S3). Together, the relative
151 contribution of different subsets to human T cells in NSGW41hIL7 mice resembled the
152 contribution in human peripheral blood. Next, we analyzed T cell receptor (TCR)
153 repertoire diversity using next-generation sequencing to assess possible post-thymic
154 peripheral expansion of T cells. This analysis revealed a high frequency of rare T cell
155 clones, which were comparable between NSGW41 and NSGW41hIL7 mice. Virtually
156 no expanded clones were observed, indicating the absence of hIL-7-induced
157 lymphoproliferation (Fig. 3c). We conclude from these data that elevated peripheral
158 frequencies of human T cells in NSGW41hIL7 mice are largely generated through
159 enhanced intrathymic T-cell differentiation. Furthermore, this route of differentiation
160 results in a composition of the peripheral T-cell compartment largely resembling human
161 peripheral blood. Paucity of peripheral lymph nodes (LN), including mesenteric (m)LN,
162 remains a critical limitation of current NSG-derived humanized mouse models. In
163 NSGW41hIL7 mice mLN were increased in number and individual size compared to
164 NSGW41 mice (Fig. 3d). Given the poor regeneration of lymph nodes in other strains
165 of humanized mice, this observation suggests that NSGW41hIL7 mice might constitute
166 an improved model for studying gut-associated immune responses. Next, we

167 characterized the functionality of conventional human T cells in NSGW41hIL7 mice.
168 To this end, we isolated and activated *ex vivo* $CD3^+$ T cells from NSGW41 or
169 NSGW41hIL7 spleens. Upregulation of the bona fide activation markers CD25 and
170 CD69 indicated similar levels of activation (Fig. S4a). Finally, NSGW41hIL7-derived
171 $CD4^+$ and $CD8^+$ T cells displayed increased divisions in response to anti-CD3/CD28 or
172 phytohemagglutinin stimulation (Fig. 3e, S4). We conclude that human T cells
173 differentiated in NSGW41hIL7 mice respond efficiently to T cell receptor triggering *ex*
174 *vivo*.
175
176 Regulatory T (Treg) cells are central in providing protection from autoreactive T cells
177 [19]. However, in the context of malignancy Treg-cell mediated immunosuppression
178 precludes effective anti-tumor immune responses [20]. Within the total T cell pool, Treg
179 cells constitute a comparatively small population, making their functional analysis
180 difficult in extant humanized mouse models with low overall T cell numbers. We
181 observed similar frequencies of regulatory T (Treg) cells in multiple organs from
182 NSGW41hIL7 or NSGW41 mice (Fig. 4a). However, given the higher overall T cell
183 numbers in NSGW41hIL7 mice, Treg cell numbers were increased making their
184 analysis feasible (Fig. 4a). To study the activation of Treg cells in humanized
185 NSGW41hIL7 mice, we transplanted porcine pancreatic islets into the portal vein of
186 humanized NSGW41hIL7 mice [4]. 18 hours after xenotransplantation, Treg cells in the
187 liver but not spleen displayed significantly increased expression of HLA-DR evidencing
188 site-specific activation through the xenograft (Fig. 4b). We conclude that humanized
189 NSGW41hIL7 mice represent a good model for the study of human Treg cells *in vivo*.
190
191 Taken together, we have demonstrated that spatially restricted expression of hIL-7 in
192 NSGW41hIL7 mice results in an improved capacity for T-cell differentiation from
193 human HSPCs. Thus, we observed T/B cell ratios geared towards a higher abundance
194 of T cells when compared to NSGW41 and other humanized mouse models [21].
195 Notably, increased intrathymic T-cell development promoted the generation of a
196 peripheral T-cell pool with a high TCR diversity and an overall composition of T-cell
197 subpopulations reminiscent of human peripheral blood. Nevertheless, thymus size and
198 cellularity in humanized NSGW41hIL7 mice remained smaller than that of wild-type
199 mice, suggesting that additional factors, presumably depending on lymphocyte-stromal
200 cell interactions, are required to generate a normal-sized thymic microenvironment

201 after humanization. It has been shown that such a limitation can be partially overcome
202 by co-transplantation of *in vitro*-differentiated proT cells [22].
203 We detected no evidence for hIL-7-driven lymphoproliferation. We designed
204 NSGW41hIL7 mice to express hIL-7 using regulatory elements that allowed to faithfully
205 identify cells expressing mIL-7 in an earlier study [23]. Our study indicates that this
206 expression pattern and the observed levels of expression of hIL-7 are able to strike a
207 balance to overcome the limited potency of mIL-7 on human lymphocytes, while at the
208 same time avoiding detrimental effects of aberrant expression of hIL-7 [13, 14].
209 Enhanced T-cell differentiation in NSGW41hIL7 mice allowed for analysis of T cell
210 subsets, including Treg cells. In addition, size and number of mLN were increased.
211 Thus, humanized NSGW41hIL7 mice have the potential to foster investigation of rare
212 human T-populations in vivo as well as gut-associated immunity.
213
214 Methods
215 Generation of NSGW41hIL7 mice: NODhIL7 mice were generated by pronuclear
216 injection of a BAC containing codon-optimized cDNA of *hIL7* introduced at the 3' end
217 of the 5'UTR of the *Il7* gene flanked by 96kb upstream, and the entire *Il7* locus plus an
218 additional 17kb downstream. The BAC was constructed according to a described
219 strategy [23]. BAC integrity upon integration and copy numbers were determined by
220 PCR. Offspring showing detectable expression of hIL-7 mRNA was crossed with
221 NSGW41 mice [2] to generate the NSGW41hIL7 strain. All animal experiments were
222 performed in accordance with German animal welfare legislation and were approved
223 by the relevant authorities: Landesdirektion Dresden, the Thüringer Landesamt für
224 Verbraucherschutz, the Niedersächsisches Landesamt für Verbraucherschutz und
225 Lebensmittelsicherheit (LAVES), and the Regierungspräsidium Darmstadt.
226 Human HSPC transplantation: Cord blood samples were obtained from the
227 Department Obstetrics, Gynecology and Reproductive Medicine, Hannover Medical
228 School, Hannover, from the Bürgerhospital Frankfurt am Main, and from the DKMS
229 Cord Blood Bank, Dresden, and were used in accordance with the guidelines approved
230 by the ethics committees of Hannover Medical School, Frankfurt University Clinics,
231 Dresden University of Technology, and University Clinics Jena. $CD34^+$ HSPCs were
232 isolated using dual magnetic beads enrichment according to the manufacturer's
233 instructions (Miltenyi Biotech) [2]. Purities >95% were considered acceptable.
234 Contaminating T cell frequencies were routinely below 1%.

235 Flow cytometry: Analysis was performed as described before [2]. A full list of antibody
236 panels is provided in Table S1.
237 TCR repertoire analysis: After mRNA isolation (Qiagen Micro Kit), cDNA was
238 generated via the Smarter 5'RACE cDNA amplification kit (Clontech) using 4.5µl
239 mRNA input and following the recommended protocol. Complementarity-determining
240 region 3 (CDR3) regions of the human TRB locus were amplified through a gene-
241 specific primer (2µM final concentration) that targets the constant region of the beta
242 (β)-chain (GCACACCAGTGTGGCCTTTTGGG) and a primer (1µM final
243 concentration) binding to the introduced SMARTER oligonucleotide
244 (CTAATACGACTCACTATAGGGC) using the Advantage 2 PCR kit (Clontech) in a
245 50µl reaction. Both primer sequences further contain 16S Illumina overhang adapter
246 sequences. Cycling conditions were as following: 120 s 95°C; 30 times 30 s 95°C, 45
247 s 64°C, 60 s 72°C; 60 s 72°C. Generated PCR amplicons were agarose gel purified
248 (Qiagen GelExtract.) Next, PCR samples were indexed with Nextera Illumina Indices
249 reads using the Advantage 2 PCR kit (Clontech) in a 8 PCR cycle reaction and purified
250 with Agencourt AMPpure XP beads (Beckman Coulter) according to the manufacturers
251 protocol. Samples were pooled, denatured and subjected to Illumina MiSeq analysis
252 using 500 cycles and paired-end sequencing following Illumina guidelines. Sequencing
253 libraries contained 20% PhIX for library complexity. Demultiplexed Fastq files were
254 annotated to the human TRB locus via MiXCR software [18]. Individual CDR3 nucleotide
255 sequences were ranked according to their abundance within the respective samples
256 and further analyzed using VDJTools [24] and TcR [25]. TCR repertoire data are available
257 at SRA (https://www.ncbi.nlm.nih.gov/sra), accession number PRJNA606460.
258 Islet xenotransplantation: 500 IEQ (Islets Equivalent) adult pig islets or PBS were
259 transplanted in the portal vein of NSGW41hIL7 mice that were humanized 24 weeks
260 before. Islets were obtained from Goettingen minipigs (Ellgard) as described before [26,
261 27]. Human blood cell chimerism of used mice was 32-85%. Regulatory T cells were
262 analyzed 18 hours after surgery.
263 T cell co-stimulation: $hCD3^+$ T cells were isolated from the spleen of humanized
264 NSGW41 or NSGW41hIL7 mice 16 to 25 weeks after HSPC transplantation, enriched
265 using negative depletion (Miltenyi), and CPD labeled (eBioscience). 10^5 $hCD3^+$ T cells
266 were mixed with human T-Activator CD3/CD28 Dynabeads (Thermofisher, ratio 3:1)
267 or PHA (1µg/mL) in RPMI 10% FCS, 20mM L-glutamine, 10mM Hepes, 1mM Sodium

268 Pyruvate, 50µM ß-mercaptoethanol with recombinant hIL-2 (30 U/mL) and incubated
269 for 6 days (37°C, 5% CO2).
270 Statistics: Student's t tests were performed for all statistical analyses using Prism 8 for
271 MacOSX software. In all graphs *p = 0.05–0.01, **p = 0.01–0.001, and ***p = 0.001-
272 0.0001 and ****p < 0.0001; data represent the mean ± SD. Boxes and whiskers display
273 the data distribution through their quartiles.
274
275 References

276 1. Shultz, L.D. *et al.* Humanized mouse models of immunological diseases and
277 precision medicine. *Mammalian genome : official journal of the International*
278 *Mammalian Genome Society* 30, 123-142 (2019).
279 2. Cosgun, K.N. *et al.* Kit Regulates HSC Engraftment across the Human-Mouse
280 Species Barrier. *Cell Stem Cell* 15, 227-238 (2014).
281 3. Mende, N. *et al.* CCND1-CDK4-mediated cell cycle progression provides a
282 competitive advantage for human hematopoietic stem cells in vivo. *J Exp Med*
283 212, 1171-1183 (2015).
284 4. Rahmig, S., Bornstein, S.R., Chavakis, T., Jaeckel, E. & Waskow, C.
285 Humanized mouse models for type 1 diabetes including pancreatic islet
286 transplantation. *Hormone and metabolic research = Hormon- und*
287 *Stoffwechselforschung = Hormones et metabolisme* 47, 43-47 (2015).
288 5. Rahmig, S. *et al.* Improved human erythropoiesis and platelet formation in
289 humanized NSGW41 mice. *Stem Cell Reports* 7, 591-601 (2016).
290 6. Yurino, A. *et al.* Enhanced Reconstitution of Human Erythropoiesis and
291 Thrombopoiesis in an Immunodeficient Mouse Model with Kit(Wv) Mutations.
292 *Stem Cell Reports* 7, 425-438 (2016).
293 7. Nicolini, F.E., Cashman, J.D., Hogge, D.E., Humphries, R.K. & Eaves, C.J.
294 NOD/SCID mice engineered to express human IL-3, GM-CSF and Steel factor
295 constitutively mobilize engrafted human progenitors and compromise human
296 stem cell regeneration. *Leukemia* 18, 341-347 (2004).
297 8. Rongvaux, A. *et al.* Development and function of human innate immune cells in
298 a humanized mouse model. *Nat Biotechnol* 32, 364-372 (2014).
299 9. Yu, H. *et al.* A novel humanized mouse model with significant improvement of
300 class-switched, antigen-specific antibody production. *Blood* 129, 959-969
301 (2017).

302 10. Puel, A., Ziegler, S.F., Buckley, R.H. & Leonard, W.J. Defective IL7R expression
303 in T(-)B(+)NK(+) severe combined immunodeficiency. *Nat Genet* 20, 394-397
304 (1998).
305 11. Peschon, J.J. *et al.* Early lymphocyte expansion is severely impaired in
306 interleukin 7 receptor-deficient mice. *J Exp Med* 180, 1955-1960. (1994).
307 12. von Freeden-Jeffry, U. *et al.* Lymphopenia in interleukin (IL)-7 gene-deleted
308 mice identifies IL-7 as a nonredundant cytokine. *J Exp Med* 181, 1519-1526.
309 (1995).
310 13. van Lent, A.U. *et al.* IL-7 enhances thymic human T cell development in "human
311 immune system" Rag2-/-IL-2Rgammac-/- mice without affecting peripheral T
312 cell homeostasis. *J Immunol* 183, 7645-7655 (2009).
313 14. Rich, B.E., Campos-Torres, J., Tepper, R.I., Moreadith, R.W. & Leder, P.
314 Cutaneous lymphoproliferation and lymphomas in interleukin 7 transgenic mice.
315 *J Exp Med* 177, 305-316 (1993).
316 15. El-Kassar, N. *et al.* High levels of IL-7 cause dysregulation of thymocyte
317 development. *Int Immunol* 24, 661-671 (2012).
318 16. El Kassar, N. *et al.* A dose effect of IL-7 on thymocyte development. *Blood* 104,
319 1419-1427 (2004).
320 17. Matsuda, M. *et al.* Human NK cell development in hIL-7 and hIL-15 knockin
321 NOD/SCID/IL2rgKO mice. *Life science alliance* 2 (2019).
322 18. Bolotin, D.A. *et al.* MiXCR: software for comprehensive adaptive immunity
323 profiling. *Nat Methods* 12, 380-381 (2015).
324 19. Sakaguchi, S. *et al.* Regulatory T Cells and Human Disease. *Annu Rev Immunol*
325 (2020).
326 20. Yano, H., Andrews, L.P., Workman, C.J. & Vignali, D.A.A. Intratumoral
327 regulatory T cells: markers, subsets and their impact on anti-tumor immunity.
328 *Immunology* 157, 232-247 (2019).
329 21. Sippel, T.R., Radtke, S., Olsen, T.M., Kiem, H.P. & Rongvaux, A. Human
330 hematopoietic stem cell maintenance and myeloid cell development in next-
331 generation humanized mouse models. *Blood advances* 3, 268-274 (2019).
332 22. Awong, G. *et al.* Human proT-cells generated in vitro facilitate hematopoietic
333 stem cell-derived T-lymphopoiesis in vivo and restore thymic architecture. *Blood*
334 122, 4210-4219 (2013).

335 23. Repass, J.F. *et al.* IL7-hCD25 and IL7-Cre BAC transgenic mouse lines: new
336 tools for analysis of IL-7 expressing cells. *Genesis* 47, 281-287 (2009).
337 24. Shugay, M. *et al.* VDJtools: Unifying Post-analysis of T Cell Receptor
338 Repertoires. *PLoS computational biology* 11, e1004503 (2015).
339 25. Nazarov, V.I. *et al.* tcR: an R package for T cell receptor repertoire advanced
340 data analysis. *BMC bioinformatics* 16, 175 (2015).
341 26. Ludwig, B. *et al.* Favorable outcome of experimental islet xenotransplantation
342 without immunosuppression in a nonhuman primate model of diabetes. *Proc*
343 *Natl Acad Sci U S A* 114, 11745-11750 (2017).
344 27. Steffen, A. *et al.* Production of high-quality islets from goettingen minipigs:
345 Choice of organ preservation solution, donor pool, and optimal cold ischemia
346 time. *Xenotransplantation* 24 (2017).
347
348
349 Acknowledgements
350 We are grateful to Katrin Witzlau and Esther Imelmann for technical assistance and
351 management of mouse colonies. We would like to thank Dr. Ellen Richie (MD Anderson
352 Cancer Center, TX, USA) for providing BAC constructs and advice on cloning. The
353 work was supported by grants from the German Research Foundation (DFG, SFB738-
354 A7 and SFB902-B15) (to A.K.) and FOR2033-A03, TRR127-A5, WA2837/6-1,
355 WA2837/7-1 and through the project EDISCIDPROG funded by the EU ERA-Net for
356 Research Programmes on Rare Diseases, E-Rare (to C.W.).
357
358 Authorship contributions
359 E.C. planned, conducted, interpreted experiments and wrote the paper. B.S. planned,
360 conducted and interpreted experiments. S.Rah, J.B., and N.V. conducted experiments.
361 J.B., S.Rav., and I.P. conducted and interpreted experiments on TCR repertoire. U.S.,
362 J.S., S.L. and B.L. isolated and provided porcine islets for xenotransplanation. F.B.,
363 C.v.K, and A.P. provided crucial reagents. R.N. generated knock-in mice, and C.W.
364 and A.K. conceived the study, planned and interpreted experiments and wrote the
365 paper.
366
367 Disclosure of conflicts of interest
368 The authors declare that no conflicts of interest exist.

369

370 Figure legends

371 **Fig. 1: Enhanced generation of human T cells upon transfer of human HSPCs in**
372 **NSGW41hIL7 mice. a**, Scheme of BAC construct for the generation of NSGW41hIL7
373 mice. **b**, Abundance of hIL7 transcript in bone marrow (BM), spleen and thymus from
374 humanized NSGW41 or NSGW41hIL7 mice. Each dot represents an individual mouse.
375 **c**, hIL7 protein levels in thymi isolated from non-humanized NSGW41 or NSGW41hIL7
376 mice (top) and in bone marrow, thymus and serum from NSGW41 or NSGW41hIL7
377 mice that have received human HPSCs 26-38 weeks before (bottom). **d**, Scheme of
378 transplantation experiments. **e**, Kinetics of the appearance of human $CD45^+$ cells
379 ($hCD45^+$, left) and $hCD3^+$ T cells within human leukocytes (right) in the blood after
380 humanization. Each dot represents an individual mouse. **f**, Frequencies of T cells, B
381 cells and non-defined other cells of human origin in the blood of NSGW41 (n=13) or
382 NSGW41hIL7 (n=16) mice 18 weeks after humanization. Numbers on top indicate T
383 vs. B cell ratios.

384

385 **Fig. 2: Efficient and prolonged intrathymic T-cell differentiation in humanized**
386 **NSGW41hIL7 mice. a**, Numbers (top) and fold-change (bottom) of human $CD45^+$ cells
387 in thymi of humanized NSGW41 or NSGW41hIL7 mice at the indicated time points
388 after humanization. Fold-changes were calculated by dividing human $CD45^+$
389 thymocyte numbers from humanized NSGW41hIL7 mice through the thymocyte
390 numbers from humanized NSGW41 mice. This was done separately for each
391 experiment and the results pooled. **b**, Analysis of CD4 and CD8 expression on $hCD45^+$
392 thymocytes from NSGW41 or NSGW41hIL7 mice that have received human HPSCs
393 15 weeks (left) or 26 (right) weeks before. **c**, Distribution of thymocyte subsets in
394 NSGW41 or NSGW41hIL7 mice at the indicated time points after humanization. **d**,
395 Numbers of B cells subsets in the bone marrow of NSGW41 or NSGW41hIL7 mice 26
396 weeks after humanization.

397

398 **Fig. 3: hIL7-BAC transgene increases functional peripheral T cells in the absence**
399 **of excessive lymphoproliferation. a**, Human $CD4^+$ and $CD8^+$ T cells in the blood of
400 humanized NSGW41 or NSGW41hIL7 mice 26 weeks after humanization. **b**,
401 Composition of blood $CD4^+$ (top) and $CD8^+$ (bottom) T cell subpopulations 26 weeks
402 after humanization: Naïve T cells, central memory (T_{CM}), effector memory (T_{EM}), T

403 effector (T_{EFF}) and recent thymic emigrants (RTE) in NSGW41, NSGW41hIL7 mice, or
404 human blood. **c**, T cell receptor (TCR) repertoire diversity in splenic αβ T cells of
405 NSGW41 or NSGW41hIL7 mice. Clones were binned into rare ($0<X\leq0.001$), small
406 ($0.001<X\leq0.01$), medium ($0.01<X\leq0.1$) and expanded ($0.1<X\leq1$) (n=3 per group). **d**,
407 Photographs of mLN from humanized NSGW41 or NSGW41hIL7 mice isolated 26
408 weeks after humanization, or C57BL/6 controls (top). mLN number per mouse (bottom
409 left). $hCD45^+$ and $hCD3^+$ cell numbers in mLN from NSGW41 or NSGW41hIL7 mice
410 isolated 26 weeks after humanization (bottom right). **e**, Activation of human T cells from
411 NSGW41 or NSGW41hIL7 mice. Histograms depict division of CDP-labeled spleen
412 $hCD3^+$ T cells 6 days after stimulation with CD3/28 beads or control (w/o, left).
413 Frequencies of non-divided human T cells and T cells that have divided 4, 5 or 6 times
414 6 days after stimulation with CD3/28 antibody-coated beads or controls (right). Top:
415 $CD4^+$ T cells, bottom: $CD8^+$ T cells.
416
417 **Fig. 4: Efficient generation of human Treg cells in NSGW41hIL7 mice. a**,
418 Representative dot plots analyzing mesenteric lymph nodes (mLN) and blood (left) and
419 numbers (right, top) and frequencies (right, bottom) of Tregs in mLN, blood, spleen
420 and liver of humanized NSGW41 or NSGW41hIL7 mice. **b**, Human activated Tregs
421 after intraportal xenotransplantation of porcine pancreatic islets into NSGW41hIL7
422 mice 26 weeks after humanization. Representative dot plots of liver and spleen
423 analysis (left). Frequencies of $HLA\text{-}DR^+$ $FoxP3^+$ T cells in spleen and liver of
424 humanized NSGW41hIL7 mice (right) 18 hours after transplantation of islets (iTx) or
425 PBS.
426

Figure 1

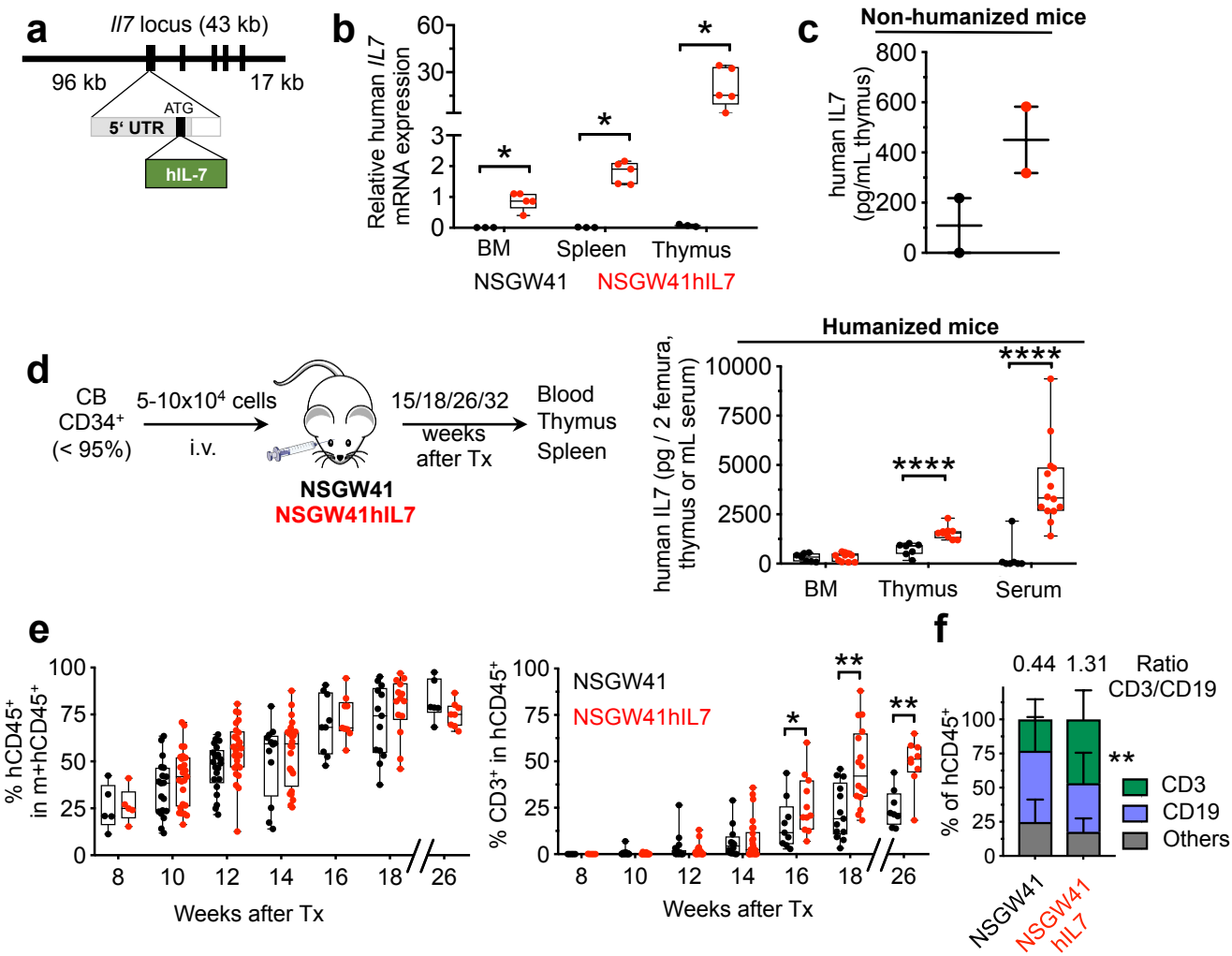
a
Il7 locus (43 kb)
96 kb
17 kb
ATG
5' UTR
hIL-7
b
Relative human IL7 mRNA expression
BM
Spleen
Thymus
NSGW41
NSGW41hIL7
c
Non-humanized mice
human IL7 (pg/mL thymus)
d
CB CD34+ (< 95%)
5-10x10^4 cells
i.v.
15/18/26/32 weeks after Tx
Blood
Thymus
Spleen
NSGW41
NSGW41hIL7
Humanized mice
human IL7 (pg / 2 femura, thymus or mL serum)
BM
Thymus
Serum
e
% hCD45+ in m+hCD45+
Weeks after Tx
% CD3+ in hCD45+
NSGW41
NSGW41hIL7
f
0.44 1.31 Ratio CD3/CD19
% of hCD45+
CD3
CD19
Others
NSGW41
NSGW41 hIL7

Figure 2

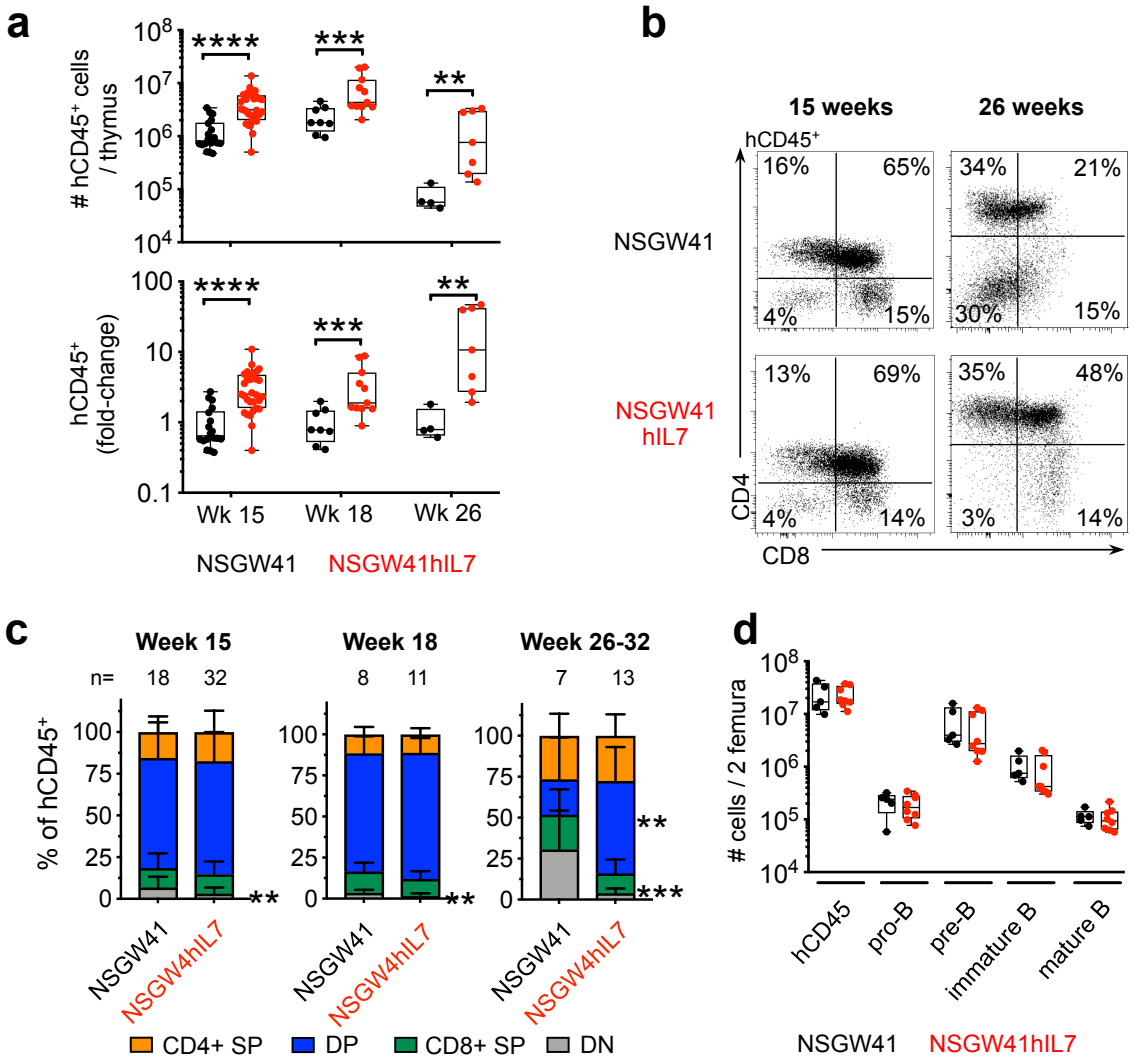
a
hCD45+ cells / thymus
hCD45+ (fold-change)
Wk 15
Wk 18
Wk 26
NSGW41
NSGW41hIL7
b
15 weeks
26 weeks
hCD45+
NSGW41
NSGW41 hIL7
CD4
CD8
16%
65%
4%
15%
34%
21%
30%
15%
13%
69%
4%
14%
35%
48%
3%
14%
c
Week 15
Week 18
Week 26-32
n=
18
32
8
11
7
13
% of hCD45+
NSGW41
NSGW4hIL7
CD4+ SP
DP
CD8+ SP
DN
d
cells / 2 femura
hCD45
pro-B
pre-B
immature B
mature B
NSGW41
NSGW41hIL7

Figure 3

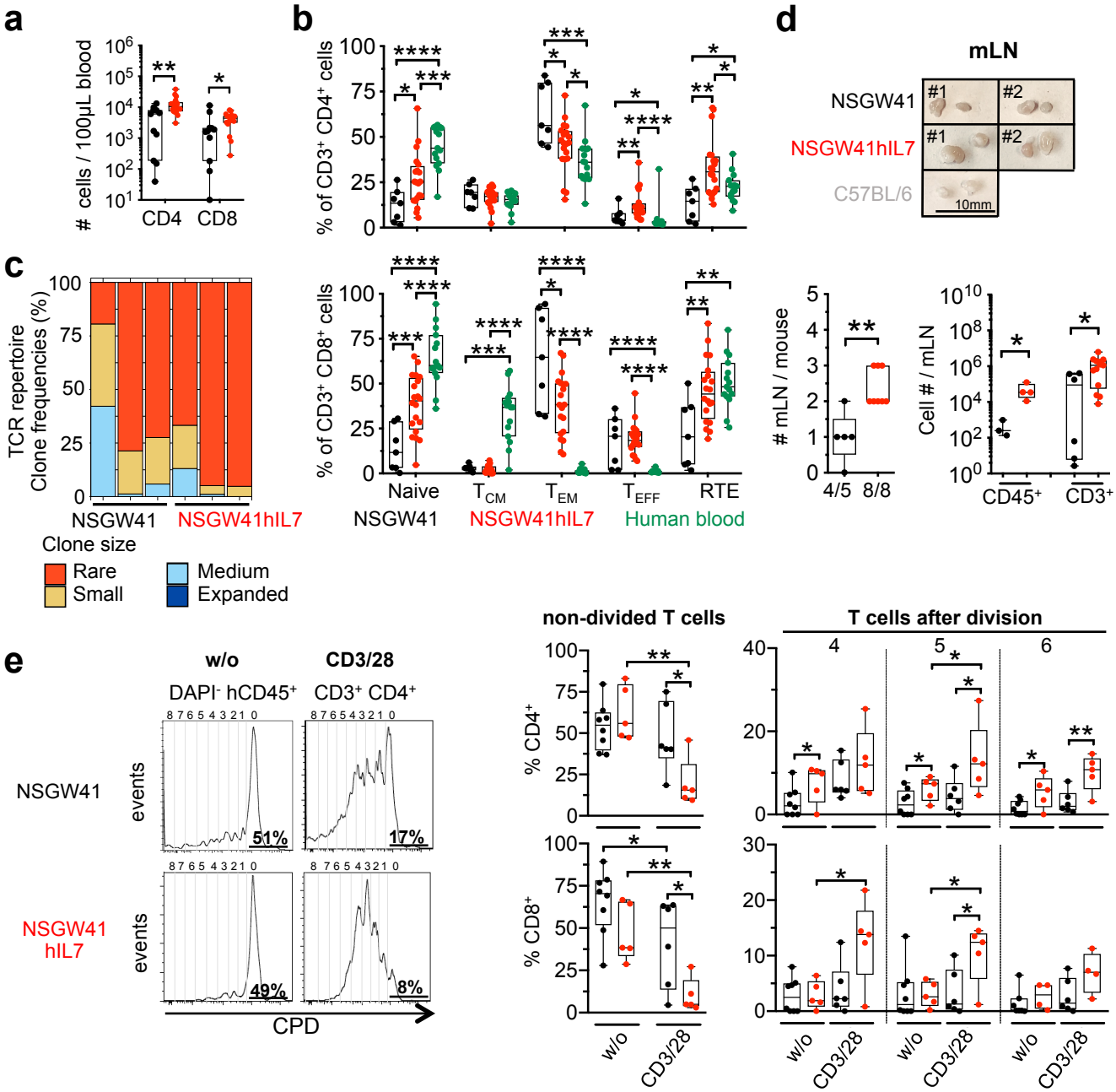
a
cells / 100µL blood
CD4
CD8
b
% of CD3+ CD4+ cells
% of CD3+ CD8+ cells
Naive
TCM
TEM
TEFF
RTE
NSGW41
NSGW41hIL7
Human blood
c
TCR repertoire
Clone frequencies (%)
NSGW41
NSGW41hIL7
Clone size
Rare
Small
Medium
Expanded
d
mLN
NSGW41
NSGW41hIL7
C57BL/6
#1
#2
10mm
mLN / mouse
4/5
8/8
Cell # / mLN
CD45+
CD3+
e
w/o
CD3/28
DAPI- hCD45+
CD3+ CD4+
events
51%
17%
49%
8%
CPD
non-divided T cells
T cells after division
% CD4+
% CD8+
w/o
CD3/28

Figure 4

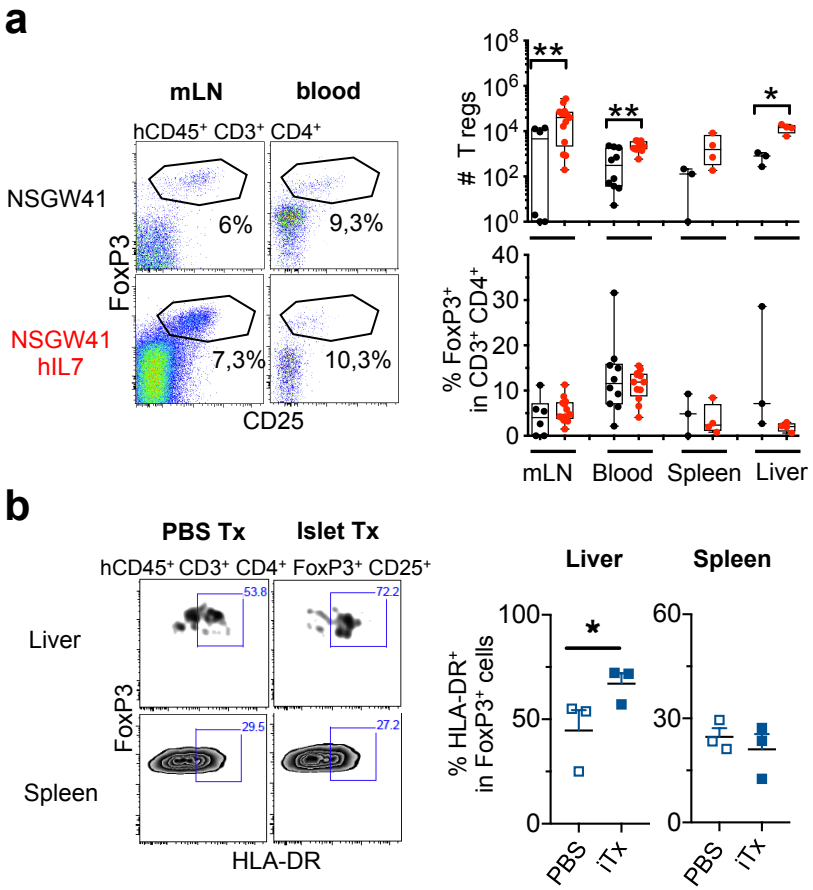
a
mLN
blood
hCD45+ CD3+ CD4+
NSGW41
NSGW41
hIL7
6%
9,3%
7,3%
10,3%
FoxP3
CD25
T regs
% FoxP3+ in CD3+ CD4+
mLN
Blood
Spleen
Liver
b
PBS Tx
Islet Tx
hCD45+ CD3+ CD4+ FoxP3+ CD25+
Liver
Spleen
53.8
72.2
29.5
27.2
FoxP3
HLA-DR
Liver
Spleen
% HLA-DR+ in FoxP3+ cells
PBS
iTx
PBS
iTx

Supplemental Material

Enhanced differentiation of functional human T cells in NSGW41 mice with tissue-specific expression of human interleukin-7.

Emilie Coppin[1,2*], Bala Sai Sundarasetty[3*§], Susann Rahmig[1,2], Jonas Blume[4], Nikita A. Verheyden[3], Franz Bahlmann[5], Sarina Ravens[4], Undine Schubert[9,10], Janine Schmid[9,10], Stefan Ludwig[11], Constantin von Kaisenberg[6], Alexander Platz[7], Ronald Naumann[8], Barbara Ludwig[9,10], Immo Prinz[4], Claudia Waskow[1,2,9,12$], Andreas Krueger[3$]

12 Table S1

13

Antibodies	Clone	Provider
CD3 APC, AF780, APC Cy7	UCHT1, HIT3a	eBioscience
CD4 PE Cy7, Pacific Blue	OKT-4/RPA-T4	eBioscience
CD8 PE Cy5, PerCP, PE Cy7	SK1, HIT8a	eBioscience
CD10 APC Cy7	HI10a	BioLegend
CD14 AF700	M5E2	BD Pharmingen
CD16 PerCP, PE Cy5	3G8	BioLegend, BD Biosciences
CD19 FITC, PC7, APC, FITC	HIB19	eBioscience
CD25 PE	M-A251	BioLegend, BD Biosciences
CD31 PE	MEM-05	Immunotools
CD33 PE, PE Cy7	WM-53	eBioscience
CD34 PE Cy7, Pacific Blue	OKT-4/RPA-T4	eBioscience
mCD45 AF780, AF700	RA3-6B2	eBioscience
hCD45 eF450, FITC, PE Cy7, PerCP	HI30	eBioscience, BioLegend
CD45RA eF450	HI100	eBioscience
CD45RO FITC, PE	UCHL1	BD Biosciences
CD62L Biotin	DREG.55	eBioscience
CD69 PerCP Cy5.5	Y1/82A	BioLegend
CD197 APC, BV510	REA337, G043H7	Miltenyi
CD235 FITC	GA-R2 (HIR2)	eBioscience
Foxp3 APC	PCH101	eBioscience
HLA DR PerCP Cy5.5	4S.B3	BioLegend
IgD PE	IA6-2	BD Pharmingen
IgM Biotin	SA-DA4	BioLegend
Ter119 FITC	11-5921-82	eBioscience
Streptavidin V500, FITC	na	BD Biosciences, BD Pharmingen
Cell Proliferation Dye eF450	na	ebioscience
Fixabe viability dye AF700	na	BD Biosciences

14

15

16 **Supplementary figures**

17

18

19

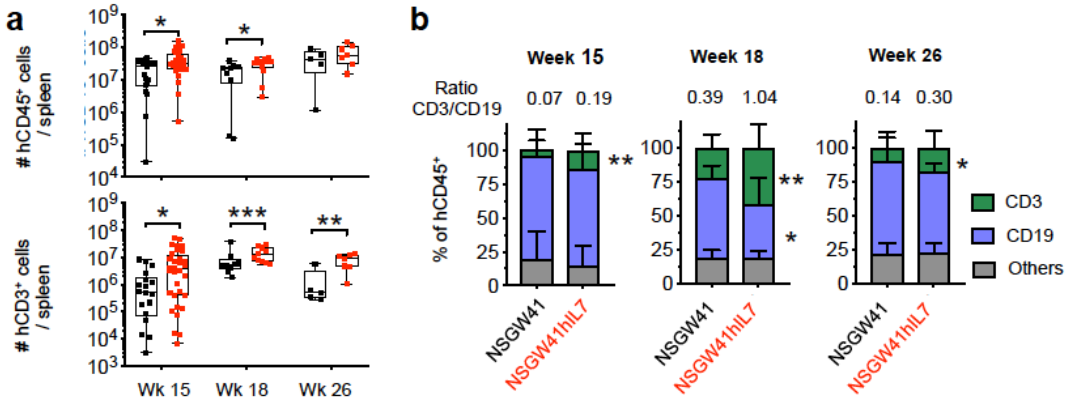

20

21

22 **Supplementary Figure 1: Human lymphocyte composition in spleen.** (**a**)
23 Numbers of hCD45$^+$ leukocytes (top) and hCD3$^+$ T cells (bottom) in spleens of
24 NSGW41 or NSGW41hIL7 mice 15, 18 and 26 weeks after humanization. (**b**)
25 Frequencies of hCD3$^+$, hCD19$^+$, and other cells within hCD45$^+$ leukocytes in spleens
26 of NSGW41 or NSGW41hIL7 mice 15, 18 and 26 weeks after humanization.
27 Numbers on top of graphs indicate T vs. B cell ratio.

28

29

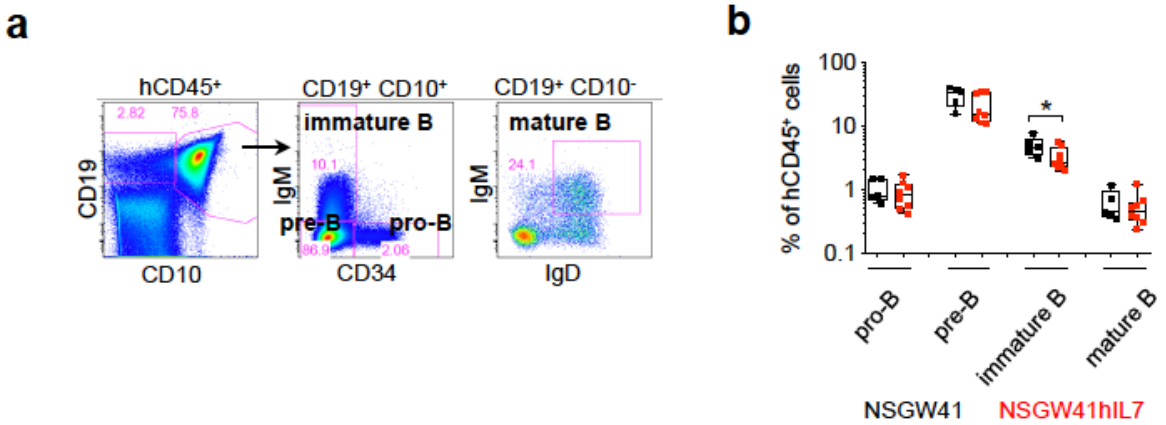

30

31 **Supplementary Figure 2: B lymphopoiesis in NSGW41hIL7 mice.** (**a**) Dot plots
32 show the gating strategy of bone marrow human B lineage subsets: pro-B (hCD45^{+}
33 CD19^{+} CD10^{+} IgM^{-} CD34^{+}), pre-B (hCD45^{+} CD19^{+} CD10^{+} IgM^{-} CD34^{-}), immature B
34 (hCD45^{+} CD19^{+} CD10^{+} IgM^{+} CD34^{-}) and mature B cells (hCD45^{+} CD19^{+} CD10^{-} IgM^{+}
35 IgD^{+}). (**b**) Frequencies of B cell subsets in bone marrow of humanized mice 26
36 weeks after humanization.

37

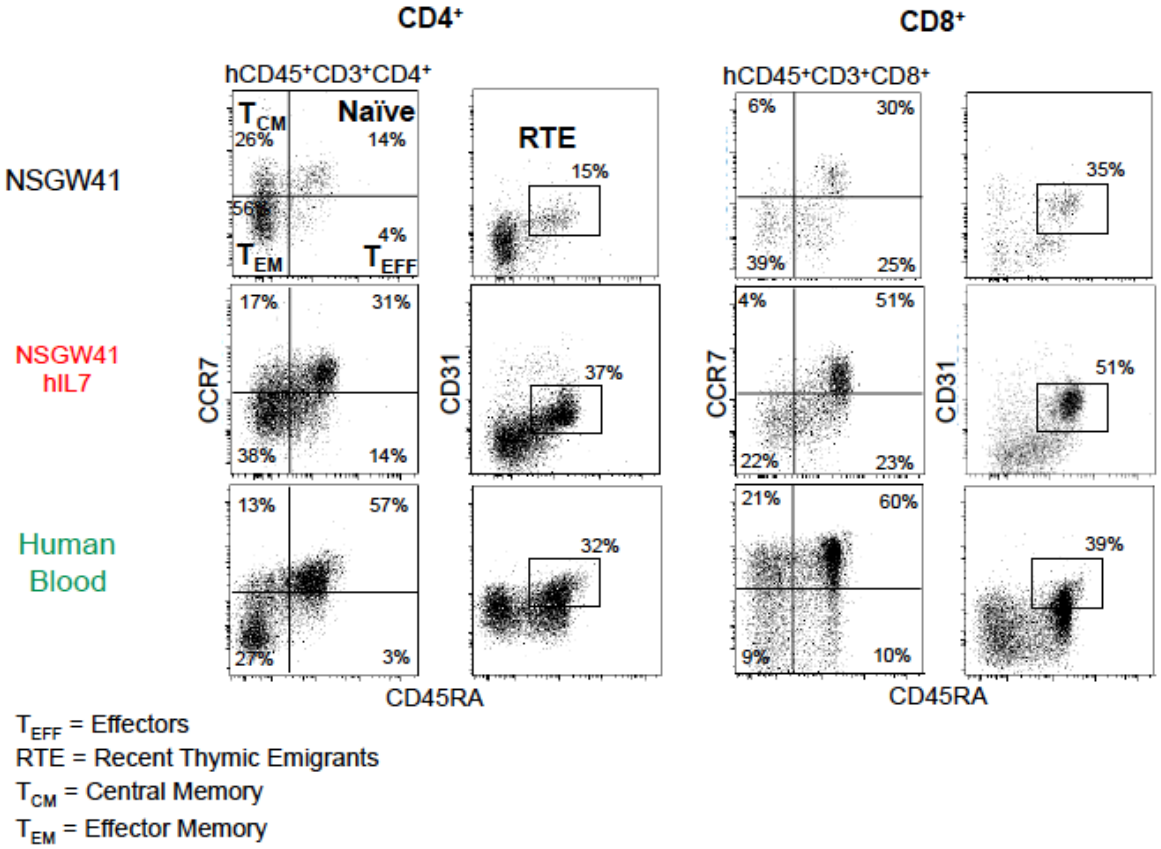

38

39 **Supplementary Figure 3: Characterization of human T cell subpopulations in**
40 **the blood.** Gating strategy and identification of hCD4$^+$ and hCD8$^+$ T cell
41 subpopulations in blood of humanized mice: T effectors (T_{EFF}, hCD45$^+$ CD3$^+$ CD4$^+$
42 CCR7$^-$ CD45RA$^+$), central memory (T_{CM}, hCD45$^+$ CD3$^+$ CD4$^+$ CCR7$^+$ CD45RA$^-$),
43 effector memory (T_{EM}, hCD45$^+$ CD3$^+$ CD4$^+$ CCR7$^-$ CD45RA$^-$), naïve T (Naïve, hCD45$^+$
44 CD3$^+$ CD4$^+$ CCR7$^+$ CD45RA$^+$) and recent thymic emigrants (RTE, hCD45$^+$ CD3$^+$ CD4$^+$
45 CD31$^+$ CD45RA$^+$). Data was acquired 26 weeks after humanization. The composition
46 of subpopulations in human blood is shown for comparison (bottom).

47

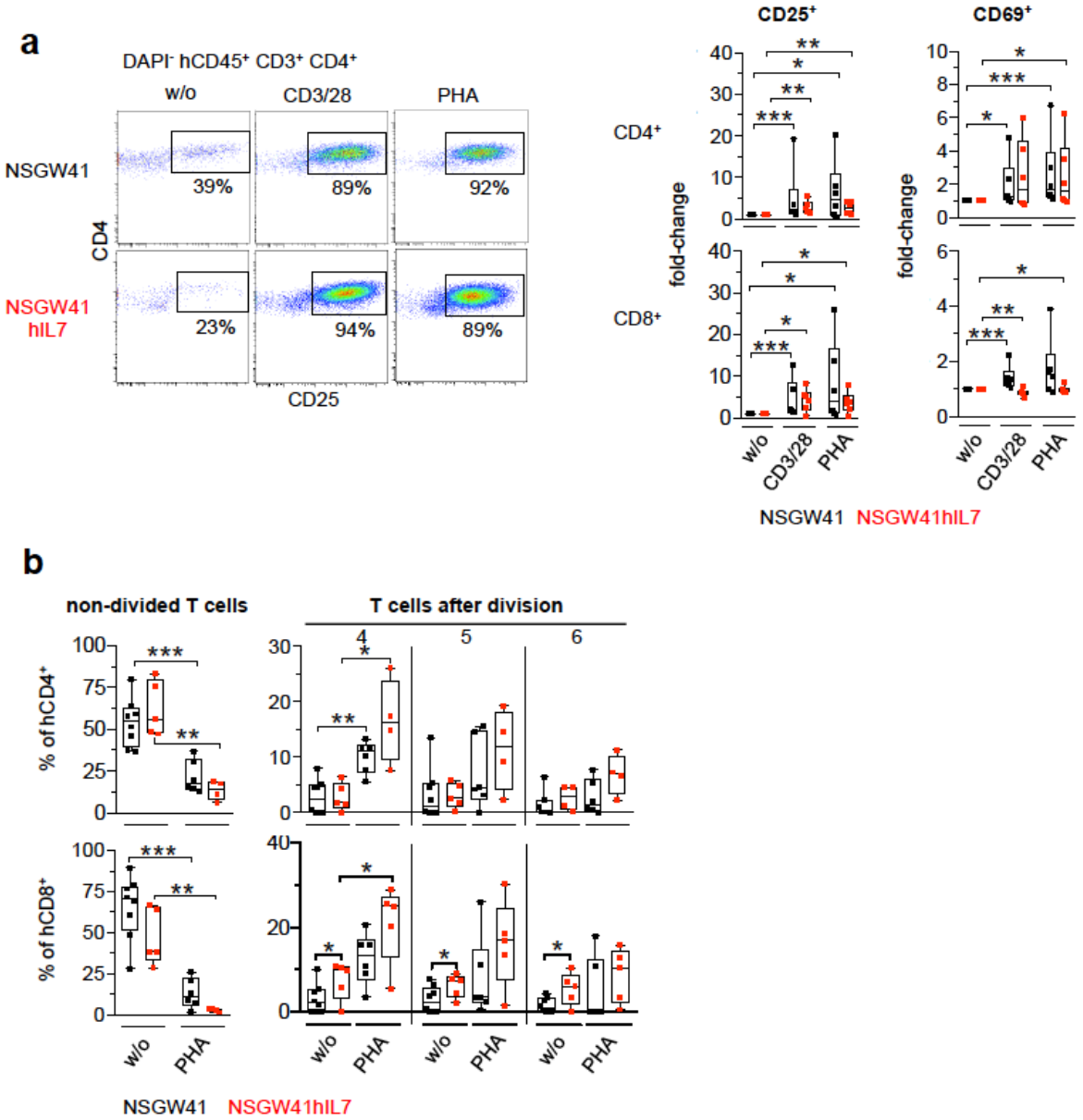

48

49 **Supplementary Figure 4: Activation of human T cells from NSGW41 or**
50 **NSW41hIL7 mice.** (**a**) Representative dot plots showing the expression of hCD25
51 and hCD69 on hCD3$^+$ T cells isolated from NSGW41 (top) or NSGW41hIL7 (bottom)
52 spleens after 6 days of CD3/28 or PHA stimulation or non-stimulated controls (left).
53 Donor mice had received human HSPCs 20 to 26 weeks before. Fold-changes were
54 calculated by dividing the percentages of stimulated hCD25$^+$ or hCD69$^+$ hCD4$^+$ (top)
55 or hCD8$^+$ (bottom) splenic T cells by the percentages of non-stimulated cells (w/o)
56 from NSGW41 or NSGW41hIL7 mice (right). (**b**) Percentages of non-divided T cells
57 and T cells which have undergone 4, 5 or 6 divisions 6 days after stimulation with
58 phytohemagglutinin (PHA) or without stimulation (w/o). Top: hCD4$^+$ T cells, bottom:
59 hCD8$^+$ T cells. Donor mice had received human HSPCs 20 to 26 weeks before.